# Liapunov exponents from time series

J. -P. Eckmann and S. Oliffson Kamphorst
*Département de Physique Théorique, Université de Genève, CH-1211 Genève 4, Switzerland*

D. Ruelle
*Institut des Hautes Etudes Scientifiques (IHES), F-91440 Bures-sur-Yvette, France*

S. Ciliberto
*Istituto Nazionale di Ottica, I-50125 Arcetri (Firenze), Italy*
(Received 24 April 1986)

We analyze in detail an algorithm for computing Liapunov exponents from an experimental time series. As an application, a hydrodynamic experiment is investigated.

## I. INTRODUCTION

In Ref. 1 two of us proposed a method to compute Liapunov exponents from an experimental time series. Here we report on a detailed analysis of this algorithm for numerical and laboratory experiments. Note that a very similar proposal has been made independently by Sano and Sawada.[2] In the course of the discussion, we shall also point out some divergences between Refs. 1 and 2.

Before discussing our algorithm, we briefly state what we are trying to do. A time evolution is realized, in Nature, in the laboratory, or on the computer, and it is assumed that this time evolution can be described by a differentiable dynamical system in a phase space of possibly infinite dimensions. We want to obtain Liapunov exponents corresponding to the large-time behavior of the system. On a more mathematical level, the large-time behavior defines an ergodic measure in phase space for the time evolution, and we are interested in the corresponding Liapunov exponents. For a discussion of these concepts and precise definitions see, for instance, Ref. 1. What we know is a time series $(x_i)_{1\le i\le N}$ obtained by monitoring a scalar signal for a finite time $T$ and with finite precision. Clearly, thus, there are limitations on how much we can say about the characteristic exponents—it is the aim of this paper to discuss some of these limitations. Certainly, we have to assume that the recording time $T$ is long, that the noise level is low, and that the measurements are made with good precision (viz., $10^{-3}$ or $10^{-4}$ if we want to determine one or two positive characteristic exponents). From a sufficiently good time series, one can in principle obtain all non-negative characteristic exponents, and it may or may not be possible to obtain also some negative ones (cf. Ref. 1).

A complete list of other methods for computing Liapunov exponents is given in Ref. 1. To our knowledge, the proposals in Refs. 1 and 2 are the only ones which allow a systematic computation of several Liapunov exponents.

## II. THE ALGORITHM

It is convenient to present the measured time series in the form of a sequence of integers $x_1, x_2, \ldots, x_N$, with $0\le x_i\le 10\,000$. (The choice of integer values speeds up the computation without sacrificing experimental precision.) The upper bound 10 000 is in accordance with a precision of $10^{-4}$ and can easily be modified, if required. We assume that the time interval $\tau$ between measurements is fixed, so that $x_i = x(i\tau)$. Note that the recording time is $T = N\tau$. The present paper deals specifically with the case of a scalar signal, but the method can easily be extended to multidimensional signals.

Conceptually, the algorithm (a copy of the computer program implementing this algorithm can be obtained from the authors) to be discussed involves the following steps: (a) reconstructing the dynamics in a finite dimensional space, (b) obtaining the tangent maps to this reconstructed dynamics by a least-squares fit, (c) deducing the Liapunov exponents from the tangent maps. We now consider these different steps in detail.

(a) We choose an embedding dimension $d_E$ and construct a $d_E$-dimensional orbit representing the time evolution of the system by the time-delay method.[3] This means that we define

$$\vec{\mathbf{x}}_i = (x_i, x_{i+1}, \ldots, x_{i+d_E-1}) \tag{1}$$

for $i = 1,2,\ldots,N-d_E+1$. In view of step (b), we have to determine the neighbors of $\vec{\mathbf{x}}_i$, i.e., the points $\vec{\mathbf{x}}_j$ of the orbit which are contained in a ball of suitable radius $r$ centered at $\vec{\mathbf{x}}_i$,

$$||\vec{\mathbf{x}}_j - \vec{\mathbf{x}}_i|| \le r \tag{2}$$

with

$$||\vec{\mathbf{x}}_j - \vec{\mathbf{x}}_i|| = \max_{0\le\alpha\le d_E-1} \{\,|x_{j+\alpha} - x_{i+\alpha}|\,\}\,. \tag{3}$$

The use of (3) rather than the Euclidean norm allows a fast search for the $\vec{\mathbf{x}}_j$ which satisfy (2). We first sort the $x_i$ (using "Quicksort," see, e.g., Knuth[4]) so that

$$x_{\Pi(1)} \le x_{\Pi(2)} \le \cdots \le x_{\Pi(N)}$$

and store the permutation $\Pi$ and its inverse $\Pi^{-1}$. Then, to find the neighbors of $x_i$ in dimension 1, we look at $k = \Pi^{-1}(i)$ and scan the $x_{\Pi(s)}$ for $s = k+1, k+2, \ldots$ until $x_{\Pi(s)} - x_i > r$, and similarly for $s = k-1, k-2, \ldots$.

 

For an embedding dimension $d_E > 1$, we first select the values of $s$ for which $|x_{\Pi(s)} - x_i| \leq r$, as above, and then impose the further conditions

$$|x_{\Pi(s)+\alpha} - x_{i+\alpha}| \leq r ,$$

for $\alpha = 1,2,\ldots,d_E - 1$.

(b) Having embedded our dynamical system in $d_E$ dimensions (it would be more correct to say that we have projected our dynamical system to $R^{d_E}$), we want to determine the $d_E \times d_E$ matrix $T_i$ which describes how the time evolution sends small vectors around $\vec{\mathbf{x}}_i$ to small vectors around $\vec{\mathbf{x}}_{i+1}$. The matrix $T_i$ is obtained by looking for neighbors $\vec{\mathbf{x}}_j$ of $\vec{\mathbf{x}}_i$ and imposing

$$T_i(\vec{\mathbf{x}}_j - \vec{\mathbf{x}}_i) \approx \vec{\mathbf{x}}_{j+1} - \vec{\mathbf{x}}_{i+1} . \tag{4}$$

The vectors $\vec{\mathbf{x}}_j - \vec{\mathbf{x}}_i$ may not span $R^{d_E}$ (think, for instance, of an embedding of the three-dimensional Lorentz system in four dimensions). Therefore, the matrix $T_i$ may only be partially determined. This indeterminancy does not spoil the calculation of the positive Liapunov exponents, but is nevertheless a nuisance because it introduces parasitic exponents which confuse the analysis, in particular with respect to zero or negative exponents which otherwise might be recoverable from the data. The way out of this difficulty is to allow $T_i$ to be a $d_M \times d_M$ matrix with a matrix dimension $d_M \leq d_E$, corresponding to the time evolution from $\vec{\mathbf{x}}_i$ to $\vec{\mathbf{x}}_{i+m}$.

Specifically, we assume that there is an integer $m \geq 1$ such that

$$d_E = (d_M - 1)m + 1 , \tag{5}$$

and associate with $\vec{\mathbf{x}}_i$ a $d_M$-dimensional vector

$$\begin{aligned} \mathbf{x}_i &= (x_i, x_{i+m}, \ldots, x_{i+(d_M-1)m}) \\ &= (x_i, x_{i+m}, \ldots, x_{i+d_E-1}) , \end{aligned} \tag{6}$$

in which some of the intermediate components of (1) have been dropped. When $m > 1$ we replace (4) by the condition

$$T_i(\mathbf{x}_j - \mathbf{x}_i) \approx \mathbf{x}_{j+m} - \mathbf{x}_{i+m} . \tag{7}$$

Taking $m > 1$ does not mean that we delete points from the data file, i.e., all points are acceptable as $\mathbf{x}_j$, and the distance measurements are still based on $d_E$, not on $d_M$. Note that, in view of (6) and (7), the matrix $T_i$ has the form

$$T_i = \begin{pmatrix} 0 & 1 & 0 & \cdots & 0 \\ 0 & 0 & 1 & \cdots & 0 \\ \vdots & \vdots & \vdots & & \vdots \\ 0 & 0 & 0 & \cdots & 1 \\ a_1 & a_2 & a_3 & \cdots & a_{d_M} \end{pmatrix} .$$

If we define by $S_i^E(r)$ the set of indices $j$ of neighbors $\vec{\mathbf{x}}_j$ of $\vec{\mathbf{x}}_i$ within distance $r$, as determined by (2), then we obtain the $a_k$ by a least-squares fit

$$\sum_{j \in S_i^E(r)} \left[ \sum_{k=0}^{d_M-1} a_{k+1}(x_{j+km} - x_{i+km}) - (x_{j+d_M m} - x_{i+d_M m}) \right]^2 = \text{minimum} .$$

The least-squares fit is the most time-consuming part of our algorithm when $S_i^E(r)$ is large. We limit ourselves therefore typically to the first 30—45 neighbors of the a point. We use the least-squares algorithm by Householder.[6] This algorithm may fail for several reasons, the most prominent being that card $S_i^E(r) < d_M$. We therefore choose $r$ sufficiently large so that $S_i^E(r)$ contains at least $d_M$ elements.

In fact, we make a new choice of $r = r_i$ for every $i$. This choice is a compromise between two conflicting requirements: take $r$ sufficiently small so that the effect of nonlinearities can be neglected, take $r$ sufficiently large so that there are at least $d_M$ neighbors of $\vec{\mathbf{x}}_i$, and in fact somewhat more than $d_M$ to improve statistical accuracy.

For the specific examples discussed in Sec. IV we have selected $r$ as follows. Count the number of neighbors of $x_i$ corresponding to increasing values of $r$ from a preselected sequence of possible values, and stop when the number of neighbors exceeds for the first time $\min(2d_M, d_M + 4)$. If with this choice the matrix $T_i$ is singular, or, more generally, does not have a previously fixed minimal rank, we again increase $r_i$. It should be noted that this last criterion only seems to come into operation for time series obtained for low-dimensional computer experiments (such as maps of the interval). We stress that the singularity of $T_i$ in itself is not catastrophic for the algorithm and the first $p$ positive Liapunov exponents are not affected provided the rank of the $T_i$ is at least $p$ (which may be a lot less than $d_M$). One should thus not stop the calculation, as suggested in Ref. 2 when the map is singular, since information about the expanding direction(s) will be lost.

(c) Step (b) gives a sequence of matrices $T_i, T_{i+m}, T_{i+2m}, \ldots$. One determines successively orthogonal matrices $Q_{(j)}$ and upper triangular matrices $R_{(j)}$ with positive diagonal elements such that $Q_{(0)}$ is the unit matrix and

$$\begin{aligned} &T_1 Q_{(0)} = Q_{(1)} R_{(1)} , \\ &T_{1+m} Q_{(1)} = Q_{(2)} R_{(2)} , \\ &\cdots , \\ &T_{1+jm} Q_{(j)} = Q_{(j+1)} R_{(j+1)} , \\ &\cdots . \end{aligned} \tag{8}$$

This decomposition is unique except in the case of zero diagonal elements. Then the Liapunov exponents $\lambda_k$ are given by

$$\lambda_k m = \frac{1}{\tau K} \sum_{j=0}^{K-1} \ln R_{(j)kk} ,$$

where $K \leq (N - d_M m - 1)/m$ is the available number of matrices, and $\tau$ is sampling time step. Obviously, fewer

matrices can be taken to shorten the computing time. [See Ref. 1 for a justification of the algorithm of Eq. (8).]

## III. REMARKS ON THE ALGORITHM

(a) Let us comment again on the usefulness of taking the matrix dimension $d_M$ different from the embedding dimension $d_E$. As we have said, if $d_M$ is not sufficiently low, there is some numerical indeterminacy in the coefficients on the $T_i$ which, combined with noise, produces undesirable parasitic Liapunov exponents (examples of this phenomenon will be shown in Sec. IV). It is thus natural to take $d_M$ relatively low (a little bigger than the expected number of positive Liapunov exponents). But if one takes $d_E$ too small, the embedding (or rather projection) of the dynamics in $R^{d_E}$ would not be well defined; orbits with different directions might go through the same point. The cure is to take $d_E > d_M$. This is, admittedly, a nonrigorous prescription, and leaves some "intuitive" freedom. We try to overcome this by examining the result for several $d_M$ and $d_E$. Note that for disentangling the dynamics, the important thing is the embedding time $d_E\tau$ rather than $d_E$; this is a first indication that it is not wise to take $\tau$ very small.

(b) As already discussed, the choice of the radius $r$ at $\vec{\mathbf{x}}_i$ is a compromise between limitations due to nonlinearities and limitations due to noise. In fact, we have chosen the smallest ball around $\vec{\mathbf{x}}_i$ which contains enough neighbors for an unambiguous determination of $T_i$ (note that the algorithm becomes impractically slow when there are more than about 45 neighbors). In principle, i.e., with very good experimental data one can do a little better.

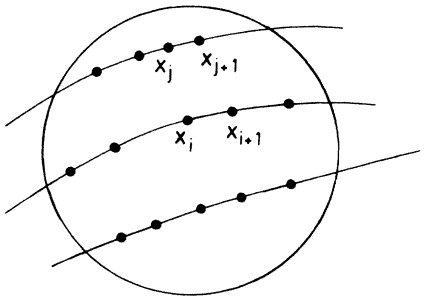


FIG. 1. Neighbors are picked up mostly on the orbit itself.

Since the effect of errors is the worst for the short vectors $\vec{\mathbf{x}}_j - \vec{\mathbf{x}}_i$ one could replace the ball

$$\{\vec{\mathbf{x}}_j:\ ||\vec{\mathbf{x}}_j - \vec{\mathbf{x}}_i|| \le r\}$$

by a shell

$$\{\vec{\mathbf{x}}_j:\ r_{\min} \le ||\vec{\mathbf{x}}_j - \vec{\mathbf{x}}_i|| \le r\}\ .$$

(c) To obtain good statistics it is, of course, desirable to have a time series with a large number $N$ of measurements. However, the really important thing is the total recording time $T = N\tau$, and increasing $N$ at fixed $T$ by making $\tau$ very small would be useless. Actually, the experimental studies of Sec. IV show that for large embedding dimension $d_E$ (hence large $r$), and small $\tau$, many of the neighbors of $\vec{\mathbf{x}}_i$ are in factor of the form $\vec{\mathbf{x}}_{i\pm1}, \vec{\mathbf{x}}_{i\pm2}, \ldots$ (see Fig. 1). Attempts at numerical projection onto the supplement of this line have given bad results.

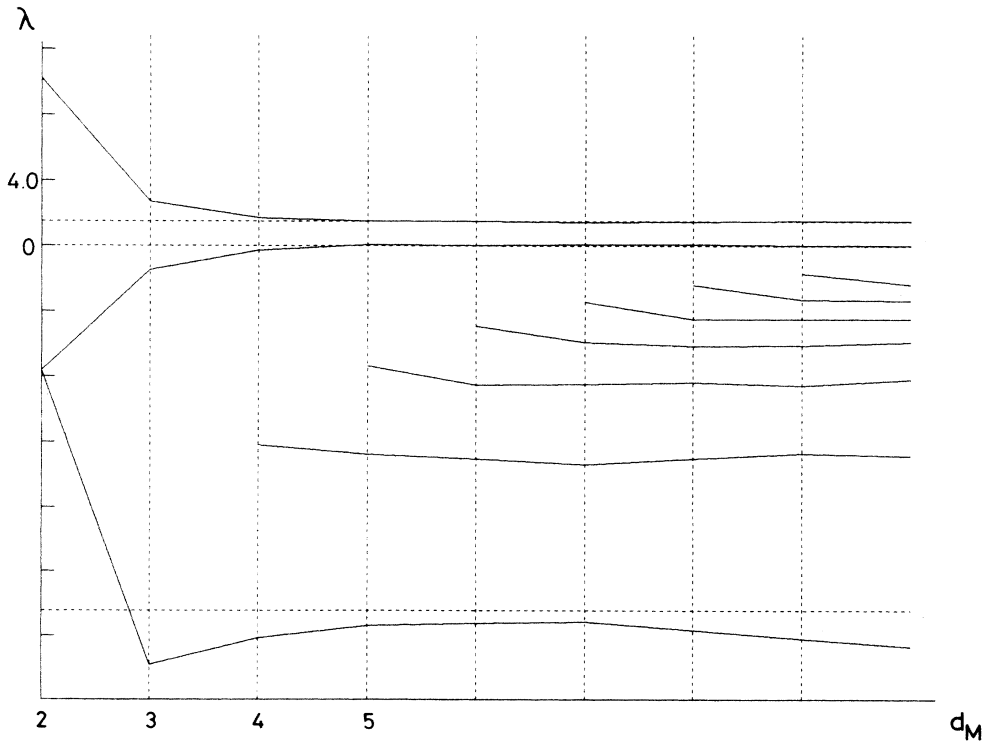


FIG. 2. The Liapunov exponents for the case $d_M = d_E$, connected in a "natural" way.

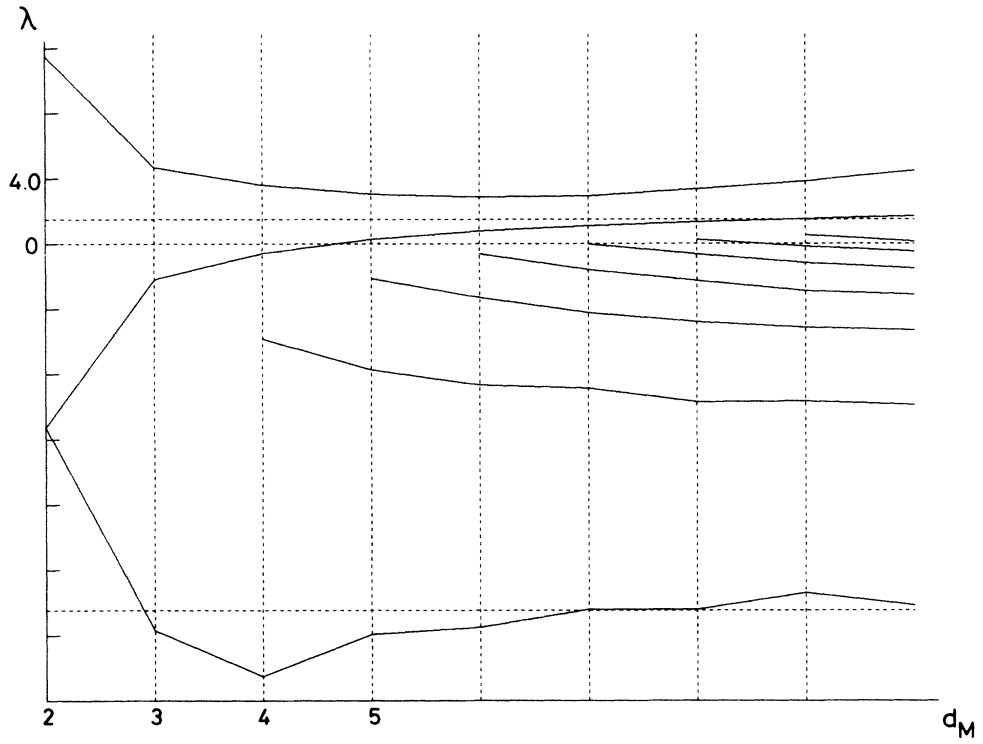


FIG. 3. Typical behavior when too few neighbors are chosen: card $S_E^i(r) \geq d_M$.

(d) Summary of advice.

(1) Use long recording time $T$, but not very small time step $\tau$.

(2) Use large embedding dimension $d_E$.

(3) Use a matrix dimension $d_M$ somewhat larger than the expected number of positive Liapunov exponents.

(4) Choose $r$ such that the number of neighbors is greater than $\min(2d_M, d_M + 4)$.

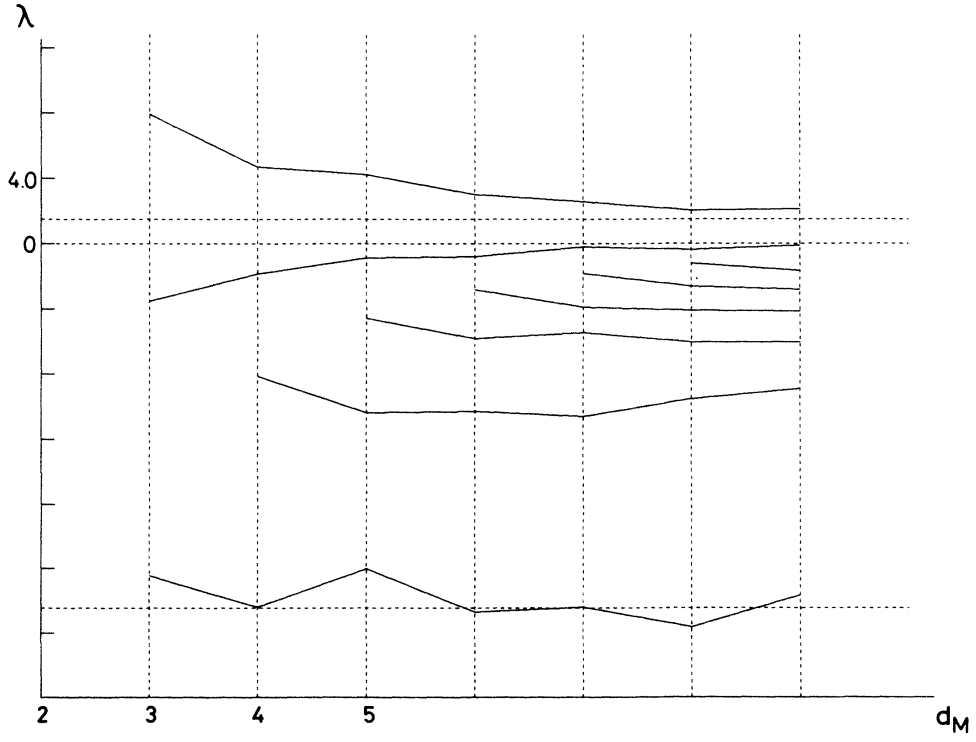


FIG. 4. A noise level of 0.4% has been added.

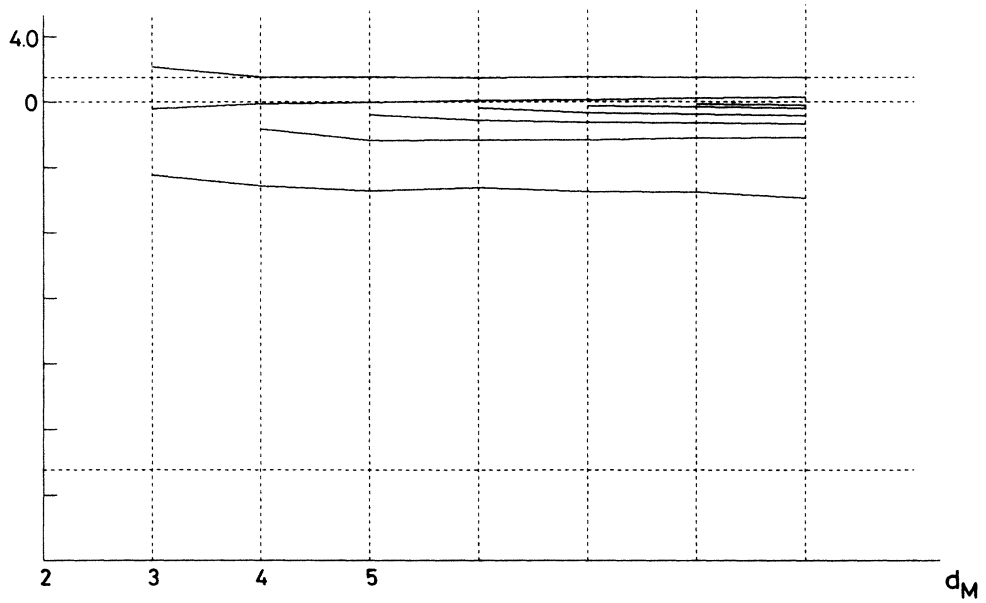


FIG. 5. The effect of the noise can be eliminated by increasing $m$ ($m=5$ for the figure).

(5) Otherwise keep $r$ as small as possible.

(6) Do not step the calculation if a singular matrix arises.

(7) Take a product of as many matrices as possible to determine the Liapunov exponents.

In particular this procedure eliminates the difficulties encountered by Vastano and Kostelich.[6]

## IV. EXAMPLES

We begin with the Lorentz equations

$$\frac{d}{dt}\begin{bmatrix} x \\ y \\ z \end{bmatrix} = \begin{bmatrix} -\sigma x + \sigma y \\ -xz + rx - y \\ xy - bz \end{bmatrix},$$

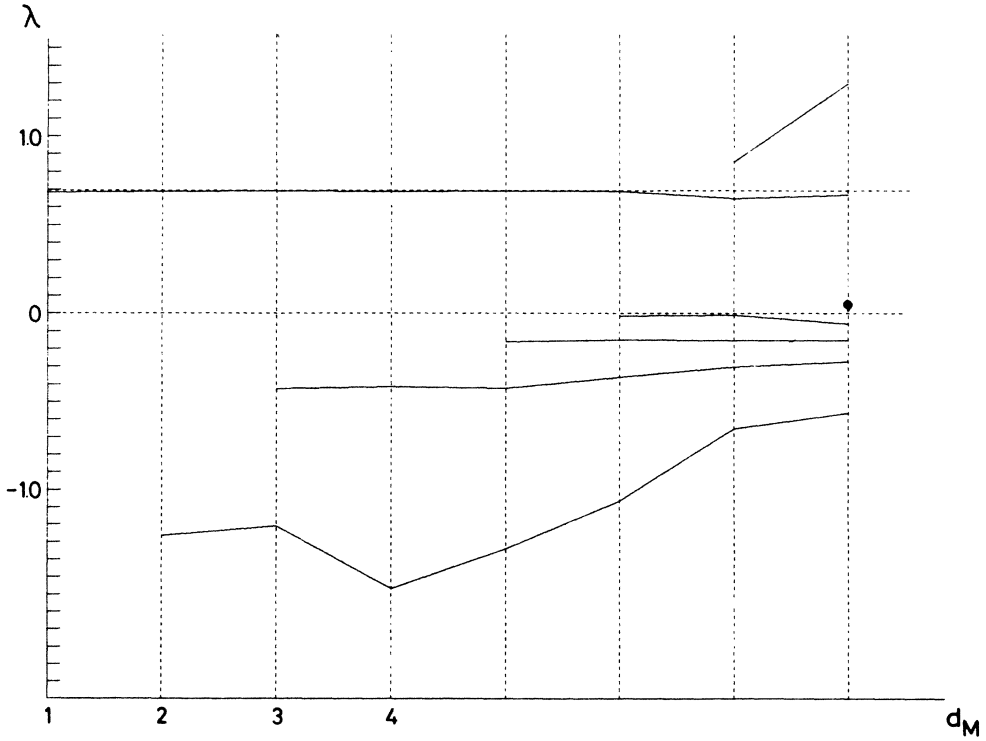


FIG. 6. Analysis of the map $x \to 1-2x^2$ with a resolution of $10^{-4}$.

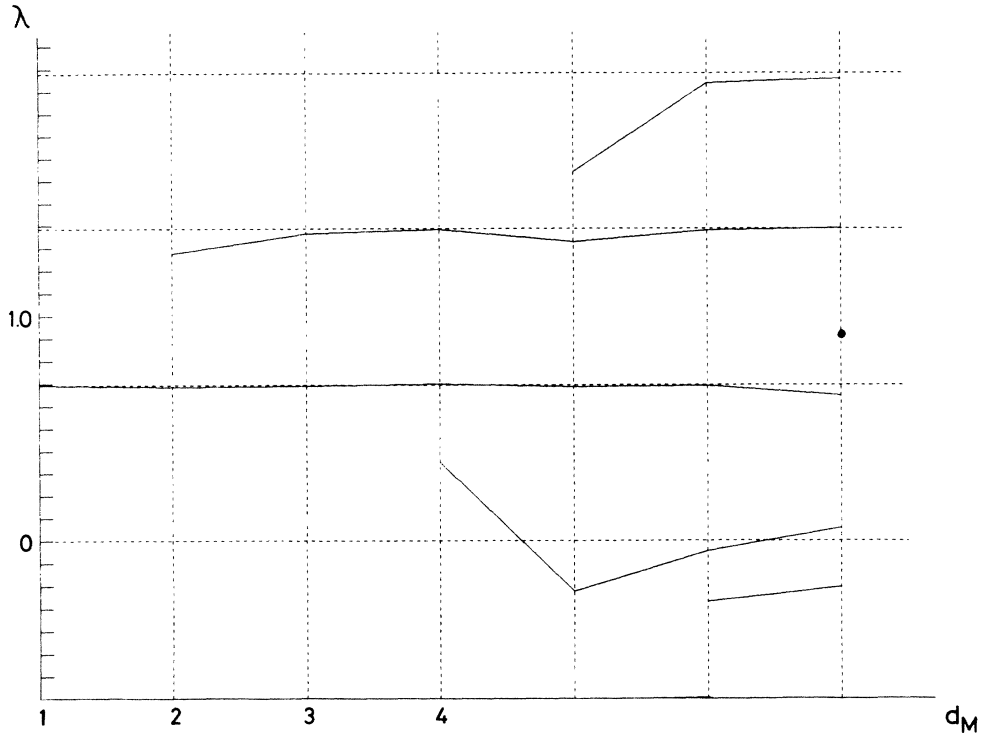


FIG. 7. Analysis of the map $x \to 1-2x^2$ with a resolution of $2^{-31}$. A spurious positive Liapunov exponent appears at $\approx 2\ln 2$.

which we study for the parameter values $\sigma=16$, $b=4$, and $r=45.92$. (These parameter values give the usual picture.) We take $\tau=0.03$ and 64 000 data points. In Fig. 2, we take $m=1$, i.e., $d_M=d_E$ and we require card $S_E^i(r)\geq 2d_M$. In this case the agreement with the numerically known non-negative Liapunov exponents (dashed lines) is very good for $d_E\geq 5$. Note that there is a large deviation at $d_E=2$. This serves as an indication that the system lives in a space with more than two dimensions. Also, as observed in Sec. III, $d_E=3$ is not a sufficiently large embedding dimension for precise values of the Liapunov exponents. Finally, it should be noted that increasing the minimal number of neighbors does not change the above observations. In Fig. 3 we illustrate the effect of taking too few neighbors. With the same parameters as in Fig. 2, we have required only card $S_E^i(r)\geq d_M$. The increase of the curves is a typical signature of a lack of sufficiently many neighbors. In Fig. 4 we analyze the influence of (artificially added) noise. We have added 0.4% noise (in terms of the total data latitude) and we observe that the prediction of the Liapunov exponent is wiped out. A typical signature of noise is the decrease of the Liapunov exponent with $d_M$. Note also that the effect of the noise can be essentially eliminated if we increase $m$, that is by increasing $d_E$ while keeping $d_M$ fixed. This is shown in Fig. 5, where we have chosen $m=5$ and card $S_E^i(r)\geq d_M+4$. The results are usually good for the positive Liapunov exponents, but the zero exponent tends to increase with $d_M$. The collection of Figs. 2–5 is a clear illustration of the summary of advice of Sec. III.

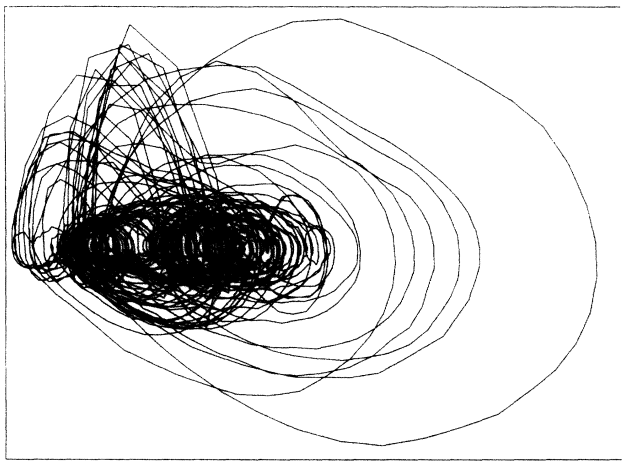

FIG. 8. An experimental orbit. Horizontal axis is $x_i$, vertical axis $x_i-x_{i-1}$.

We next illustrate in more detail the effect of having too few data points. For this we shall deal with the very simple system defined by the map $x\to 1-2x^2$ of the interval $(-1,1)$. It has a Liapunov exponent ln2. Figure 6 shows the results analogous to Fig. 2, with a resolution of the data of $10^{-4}$ (obtained by multiplying each $x$ by 5000 and truncating). To make the statistical errors smaller, we have insisted on a minimum of 20 neighbors per point. In Fig. 7 we have applied the same algorithm, but with a precision of $2^{-31}\approx 0.5\times 10^{-9}$. While this situation is unlikely to occur in laboratory experiments, it is typical for the appearance of spurious Liapunov exponents which are

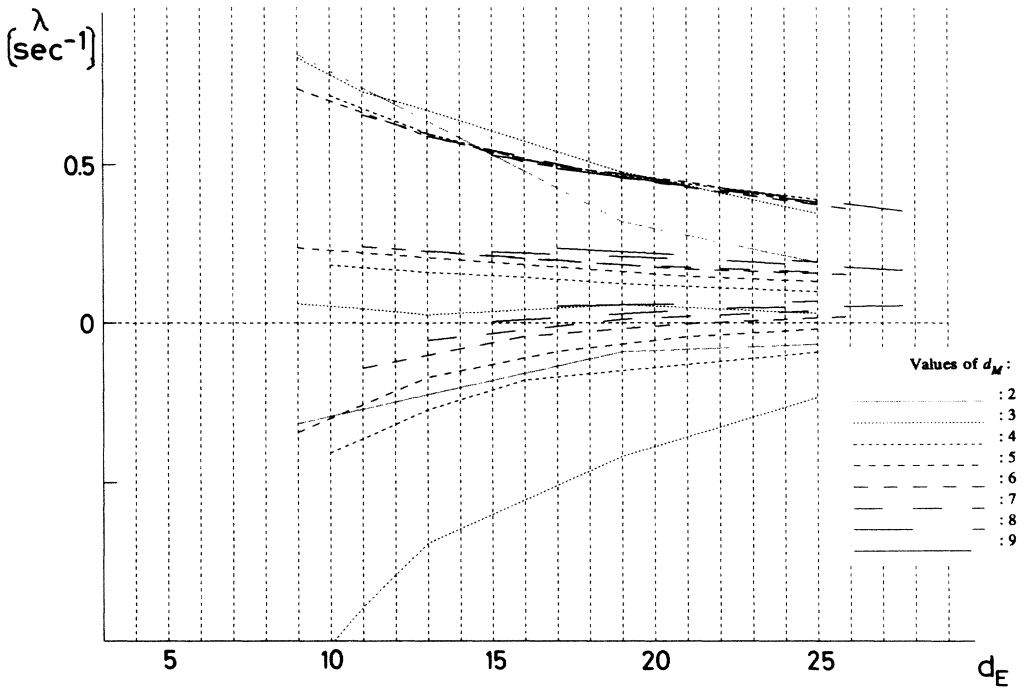


FIG. 9. Largest three Liapunov exponents as a function of $d_E$ for the signal of Fig. 8, for different values of $d_M$.

about twice (in principle even thrice) the real ones. This phenomenon is generated by the finiteness of the data set. This means that we cannot achieve the limit $r \to 0$ to determine the matrices $T_i$. Therefore one expects the nonlinearities to be important. A simple calculation shows that if one carries along second-order effects in the equations leading to the $T_i$, for the map $x \to 1-2x^2$ in dimension $d_M = 2$, one obtains two Liapunov exponents, one at ln2 and one at 2 ln2. In the absence of noise, the nonlinear terms desingularize the equations for the $T_i$ when $d_M$ is larger than the true dimension of the system, and they tend to generate multiples of the "true" Liapunov ex-

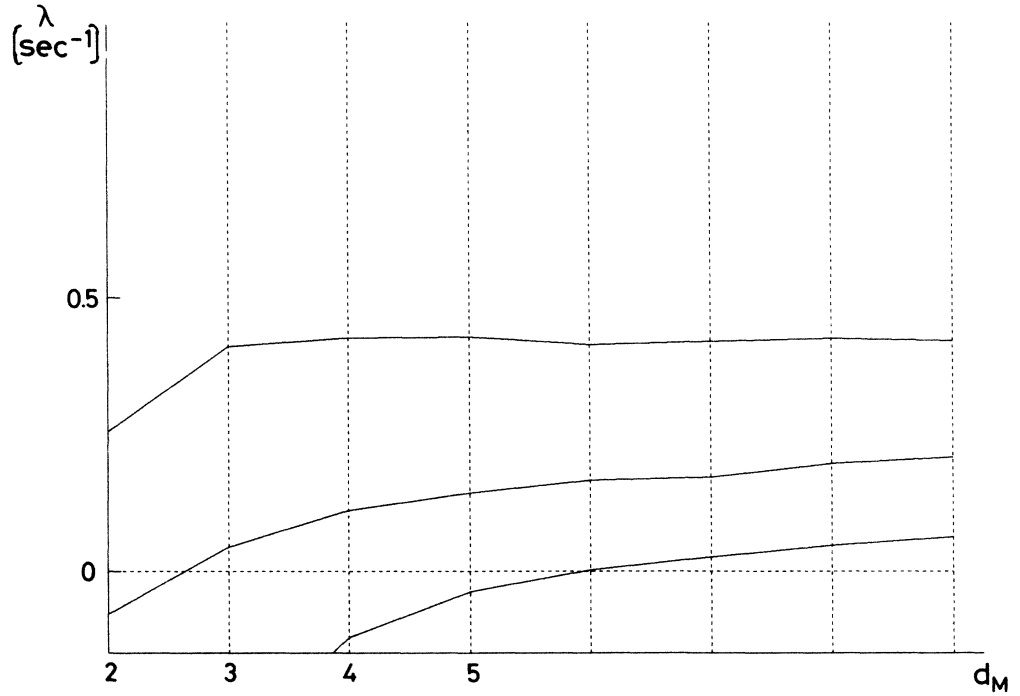


FIG. 10. Liapunov exponents as a function of $d_M$ at fixed $d_E = 22$.

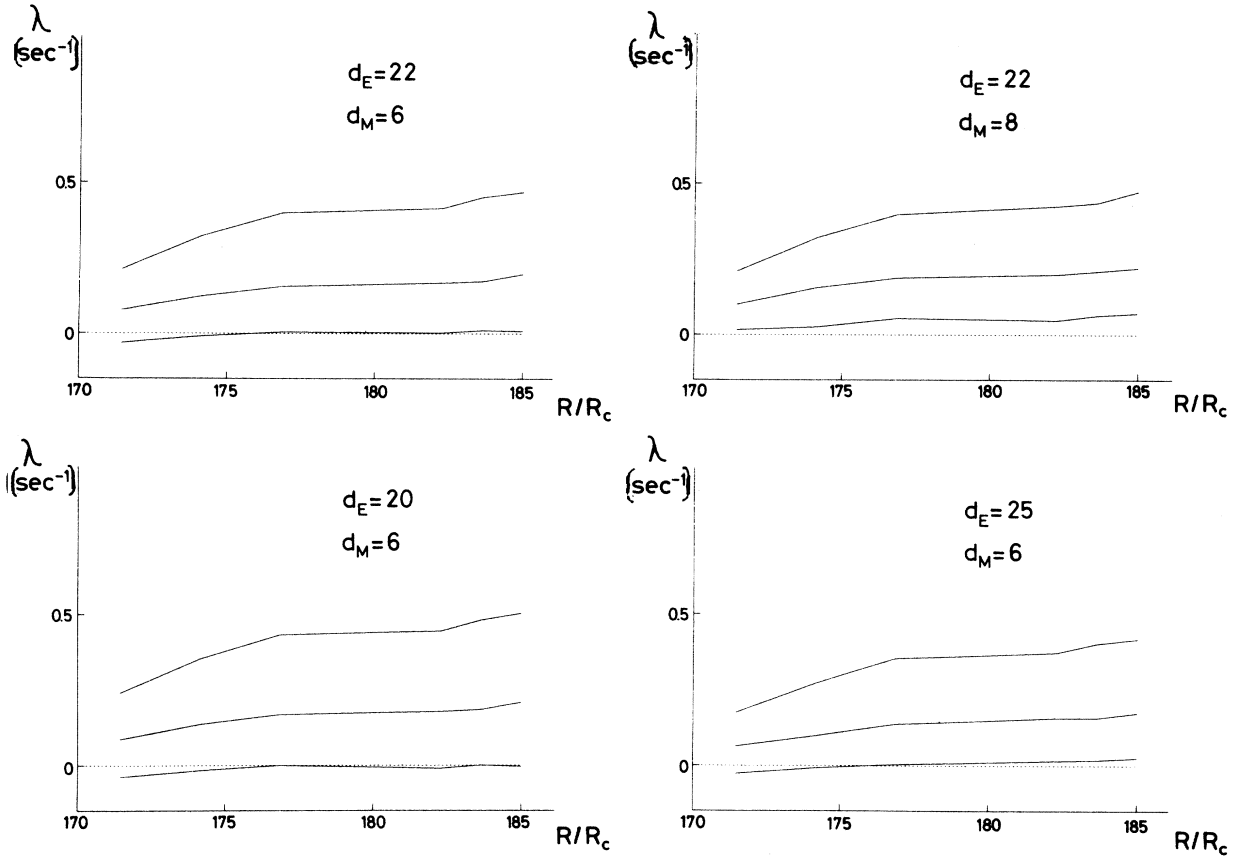


FIG. 11. Three largest Liapunov exponents as a function of Rayleigh number, for different $d_M$ and $d_E$. From theoretical arguments we know that one Liapunov exponent is equal to zero.

ponents. Having gone to very high precision in the calculations leading to Fig. 7, we have produced explicitly the generation of a "double" Liapunov exponent. (We suspect that Table I in Ref. 5 has the same origin.) In third-order terms are above the numerical imprecision one will in principle see a "triple" Liapunov exponent, and so on. For data coming from laboratory experiments, the equations for the $T_i$ are in general rather desingularized by the noise of the data. In that case a model calculation can be done, based on some independence assumptions of the noise (which may not be justified in general). For the map $x \to 1-2x^2$ and $d_M=2$, this calculation predicts that the two Liapunov exponents will be ln2 and $\approx -1.2$.

Let us summarize. All of the above effects only concern the spurious Liapunov exponents, because they are caused by the desingularization of the equations for the $T_i$. If the noise is not too small relative to the precision and the density of the data, one will see the true Liapunov exponents and the spurious ones will all be negative. This seems to be the usual situation in laboratory experiments.

We now discuss the more difficult problem of analyzing an experimental time series. In particular, we have made measurements coming very close to the required desiderata of Sec. III. In this section we only analyze one of these runs, from the same point of view as the numerical experiments. In the Appendix, the experiments and the complete results are described, as function of a varying parameter. To give a certain feeling of what is involved, we draw a piece of the experimental orbit (Fig. 8).

In Fig. 9 we summarize the results of varying the lags $m$ and matrix dimension $d_M$ in such a way that $d_E$ varies between 9 and 26. We limit $d_M$ between 2 and 9. One observes a relatively flat section in the region above $d_E=20$ for $d_M>3$. This limit is more visible in Fig. 10, where we plot, by interpolation, a section of Fig. 8 at $d_E=22$. In view of the preceding discussions, we conclude that there are two positive Liapunov exponents. In the Appendix, we show the complete results for a series of experiments with varying parameters. (The main body of this paper was done by the first three authors, and the experiment, as well as the Appendix, have been provided by the fourth author. Our collaboration has made an optimization of the experiment and the analysis possible.)

*Noted added in proof.* An interesting recent paper by A. M. Fraser and H. L. Swinney [Phys. Rev. A 33, 1134 (1986)] indicates how to choose time delays optimally in the reconstruction of dynamics from a time series. For other general literature see Ref. 1, which contains in particular a reference to a paper by Wolf *et al.* We remain unconvinced that the method described in that paper allows the systematic computation of several Liapunov exponents from noisy experimental data.

## ACKNOWLEDGMENTS

This work has been made possible by various institutions and organizations. We gratefully acknowledge the support of Institut des Hautes Etudes Scientifique (IHES), Bures-sur-Yvette (JPE), Coordenacão de Aperfeicoamento de Pessoal do Ensino Superior (CAPES), Brazil (SOK), Fonds National Suisse (DR,SC), European Economic Community Contract STI-082-J-C(CD), (SC).

## APPENDIX

The transition from a regular to a chaotic behavior has been widely studied both theoretically and experimentally in many physical, chemical, and other natural phenomena. In fluid mechanics one of the most used systems to investigate the onset of turbulence is thermal convection in a horizontal fluid layer heated from below, that is, Rayleigh-Benard convection (RB).[7] When the fluid is confined in a cell whose horizontal dimensions are of the same order of the fluid height (small aspect ratio cells), it has been found that the transition to the chaotic behavior can be explained in terms of the nonlinear interaction of a small number of degrees of freedom. This has been verified either by checking if the observed route to chaos was equal to one of the standard routes to chaos for low-dimensional systems[7] or more quantitatively with the measurement of the fractal dimension of the attractor.[8,9]

In a RB experiment the determination of the positive Liapunov exponents, that are indeed an important sign of the existence of a strange attractors, has been done only in Ref. 2 with a method similar to that outlined in the previous pages. Nevertheless, as pointed out in this text, there are some differences between the two methods and so we have applied the algorithm here proposed to evaluate the Liapunov exponents from a series of data recorded in the chaotic regime of a RB cell.

The fluid layer has horizontal sizes $l_x=4$ cm, $l_y=1$ cm, and height $d=1$ cm (aspect ratios $\Gamma_x=4, \Gamma_y=1$). The fluid is silicon oil with Prandtl number 30. The bottom and top plates of the cell are made of copper and the temperature stability is about 1 mK. The lateral walls are made of glass to allow optical inspection. The detection system allows a semilocal measurement to be made. In fact, it consists of a laser beam, with a diameter of 1 mm, that crosses the fluid layer parallel to the rolls axis and is deflected by the thermal gradients inside the fluid. By measuring the deflection of the laser beam outside the cell we can measure the thermal gradient averaged along the optical path. We record the horizontal component of the gradient because it usually has the largest time-dependent amplitude.

In order to have a signal-to-noise ratio within the requirements specified in this paper, particular attention has been paid to reduce the environmental noise produced, for example, by the air convection along the optical path of the laser beam, by the vibrations of the mirrors, and of the laser cavity. Furthermore, to eliminate high-frequency noise, the signal has also been filtered at a suitable cutoff frequency to avoid that the rising time of the filter influencing the evaluation of the Liapunov exponents. This way a signal-to-noise ratio of about $10^{-4}$ has been achieved.

Analyzing the fluid behavior as a function of $R/R_c$ ($R_c$ is the critical value of the Rayleigh number), we find, except for a small region at $81<R/R_c<90$ where the convective motion is time dependent, a stable four-rolls structure for $R/R_c<141$. Above this threshold a periodic oscillation at a frequency of 75 mHz is observed. Increasing $R$, the fluid crosses many different periodic and biperiodic states and it goes into the chaotic region via intermittency at $R/R_c>170$. We have characterized this chaotic behavior by measuring the Liapunov exponents as a function of the Rayleigh number.

To satisfy all other requirements of the algorithm, 40 000 points, with a sampling frequency of 5 Hz, have been recorded for each measurement. This way, the time evolution of the system is followed for about 600 periods of the main oscillation. Many tests have been done to verify how the Liapunov exponents depend on $d_E$ and $d_M$. It has been found that the value of $\lambda$ is sufficiently stable in the interval $20<d_E<25$ and $5<d_M<8$. The results are reported in Fig. 11, where the values of the positive Liapunov exponents are shown as a function of $R$ for different $d_E$ and $d_M$. We see that the qualitative behavior of the curves is similar and the difference between them is about 10%. The measurements were done for $R/R_c=171.41$, 174.08, 176.75, 182.10, 183.44, and 184.79. Figures 8–10 show details for $R/R_c=182.10$.

By moving the detection point inside the cell by about 1 cm and keeping $R$ at the last value shown in Fig. 11 we find that the Liapunov exponents change by less than 5%. As a conclusion, the positive Liapunov exponents in the chaotic regime of a RB convection experiment have been determined using the method proposed in (Ref. 1). Even though the error of the measurement is not small (about 10%) it is still possible to follow how the number of the Liapunov exponents and their values change as a function either of the control parameter $R$ or of the position where the measurement has been taken inside the fluid.

[1]J.-P. Eckmann and D. Ruelle, Rev. Mod. Phys. **57**, 617 (1985).
[2]M. Sano and Y. Sawada, Phys. Rev. Lett. **55**, 1082 (1985).
[3]N. H. Packard, J. P. Crutchfield, J. D. Farmer, and R. S. Shaw, Phys. Rev. Lett. **45**, 712 (1980).
[4]D. E. Knuth, *The Art of Computer Programming* (Addison-Wesley, New York, 1973), Vol. 3.
[5]J. A. Vastano and E. J. Kostelich, in *Entropies and Dimensions*, edited by G. Mayer-Kress (Springer-Verlag, Berlin, in press).
[6]J. H. Wilkinson, and C. Reinsch, *Linear Algebra* (Springer-Verlag, Berlin, 1971).
[7]For a recent review, see, e.g., R. P. Behringer, Rev. Mod. Phys. **57**, 657 (1985).
[8]B. Malraison, P. Atten, P. Bergé, and M. Dubois, J. Phys. Lett. **44**, L897, (1983).
[9]M. Giglio, S. Musazzi, and V. Perini, Phys. Rev. Lett. **53**, 240 (1984).